

REPORT DOCUMENTATION PAGE

AD-A248 461



FIC

ECTE

3-9-1992

B

B

B

B

B

B

B

B

B

B

B

B

B

B

B

B

B

B

B

B

B

B

B

B

B

B

B

B

B

B

B

B

B

B

B

B

B

B

B

B

B

B

B

B

B

B

B

B

B

B

B

B

B

B

B

B

B

B

B

B

B

B

B

B

B

B

B

B

B

B

B

B

B

B

B

B

B

B

B

B

B

B

B

B

B

B

B

B

B

B

B

B

B

B

B

B

B

B

B

B

B

B

B

B

B

B

B

B

B

B

B

B

B

B

B

B

B

B

B

B

B

B

B

B

B

B

B

B

B

B

B

B

B

B

B

B

B

B

B

B

B

B

B

B

B

B

B

B

B

B

B

B

B

B

B

B

B

B

B

B

B

B

B

B

B

B

B

B

B

B

B

B

B

B

B

B

B

B

B

B

B

B

B

B

B

B

B

B

B

B

B

B

B

B

B

B

B

B

B

B

B

B

B

B

B

B

B

B

B

B

B

B

B

B

B

B

B

B

B

B

B

B

B

B

B

B

B

B

B

B

B

B

B

B

B

B

B

B

B

B

B

B

B

B

B

B

B

B

B

B

B

B

B

B

B

B

B

B

B

B

B

B

B

B

B

B

B

B

B

B

B

B

B

B

B

B

B

B

B

B

B

B

B

B

B

B

B

B

B

B

B

B

B

B

B

B

B

B

B

B

B

B

B

B

B

B

B

B

B

B

B

B

B

B

B

B

B

B

B

B

B

B

B

B

B

B

B

B

B

B

B

B

B

B

B

B

B

B

B

B

B

B

B

B

B

B

B

B

providing the most accurate information on the vertical structure of different flare tracers visible in radio wavelengths.

Accession For	
NTIS GRA&I	<input checked="" type="checkbox"/>
DTIC TAB	<input type="checkbox"/>
Unannounced	<input type="checkbox"/>
Justification	
By	
Distribution/	
Availability Codes	
Dist	Avail and/or Special
A-1	



VLA, PHOENIX and BATSE Observations of an X1 Flare

Robert F. Willson, Dept. of Physics and Astronomy, Tufts University, Medford, MA 02155
Markus J. Aschwanden, NASA/GSFC, Code 602.6, Greenbelt, MD 20771
Arnold O. Benz, Institute for Astronomy, ETH, CH-8082 Zürich, Switzerland

ABSTRACT: We present observations of an X1 flare (July 18, 1991) detected simultaneously with the Very Large Array (VLA), the PHOENIX Digital Radio Spectrometer and the Burst and Transient Source Experiment (BATSE) aboard the Gamma Ray Observatory (GRO). The VLA was used to produce snapshot maps of the impulsive burst emission on timescales of 1.7 sec at both 20 and 91 cm. Our results indicate electron acceleration in the higher corona ($h \approx 0.4 - 0.5 R_\odot$) several minutes before the onset of the hard X-ray burst detected by BATSE. Comparisons with high spectral ($\Delta\nu = 3$ MHz) and temporal ($\Delta t = 40$ ms) observations by PHOENIX reveal a variety of radio bursts at 20 cm, such as type III bursts, intermediate drift bursts, and quasi-periodic pulsations during different stages of the X1 flare. From the drift rates of these radio bursts we derive information on local density scale heights, the speed of radio excitors, and the local magnetic field. Radio emission at 90 cm shows a type IV burst moving outward with a constant velocity of 240 km/s.

The described X1 flare is unique in the sense that it appeared at the east limb (N06/E88), providing the most accurate information on the vertical structure of different flare tracers visible in radio wavelengths.

1. GOES and BATSE/GRO data

We present some preliminary data from the sofar largest flare simultaneously observed by VLA, PHOENIX and GRO, which occurred on July 18, 1991. A GOES X1-class soft X-ray event was reported near the east limb (North 06, East 88) in NOAA/USAF active region 6734, starting at 1425 UT, with maximum at 1441 UT, and ending at 1519 UT. An $H\alpha$ flare with importance 1N was detected during this time, associated with eruptive prominences and sprays.

BATSE recorded enhanced hard X-ray emission (> 25 keV) after 1425:34, which was interrupted by GRO spacecraft night from 1430:10 until 1503:00 UT, and lasted until 1510:10 UT. The BATSE hard X-ray time profile (Fig. 1) shows two peaks in the early rise of the impulsive phase, and the end of the decay phase, while most of the main flare phase was missed during spacecraft night. The major HXR peak at 1429-1430 UT is correlated with a group of fast-drifting bursts at > 1.3 GHz.

2. VLA observations

The VLA observations were made at $\nu = 1441.6$ MHz (20.8 cm) and 333 MHz (90 cm) with bandwidths of 3.25 MHz and a time resolution of 1.66 seconds. At the time of these observations, the VLA was in the A configuration which provided synthesized beamwidths of $\approx 1''$ at 20.8 cm and $\approx 5''$ at 90 cm.

92-08986



Radio emission at 90 cm indicates impulsive and relatively low-intensity bursts (10-15 SFU) beginning at 14:19 UT, or about three minutes after the first enhancements of soft X-ray emission and about six minutes before the start of the BATSE hard X-ray burst. These metric bursts are located at different locations at heights of $h = 0.4 - 0.5 R_{\odot}$ above the limb (Fig. 2). They have angular sizes of $\approx 1.5'$ and peak brightness temperatures of $T_b = 3.4 - 6.7 \times 10^7$ K.

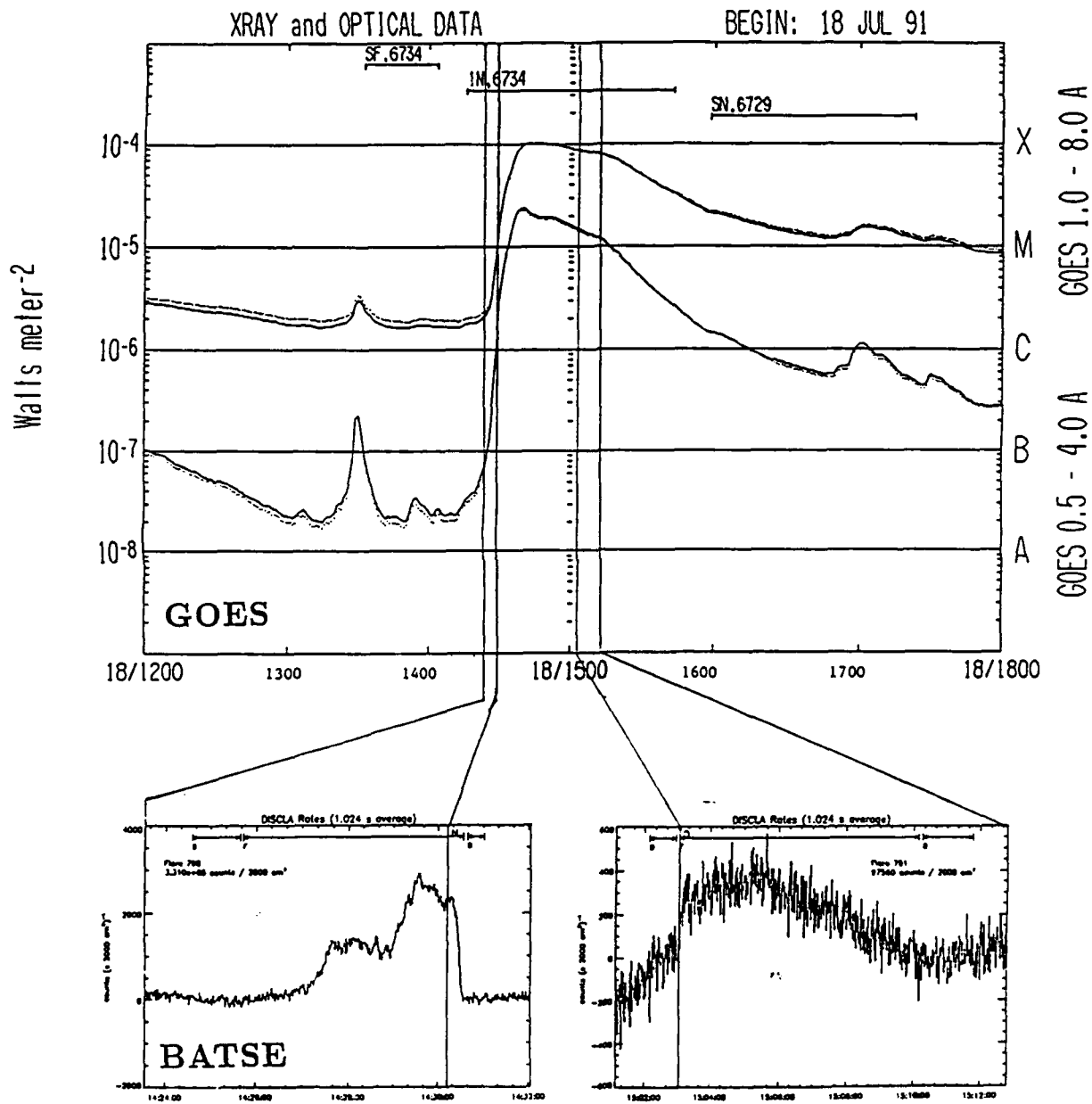


Fig. 1: Time profile of the GOES soft X-ray data (0.5-4.0 and 1.0-8.0 Angstrom) and BATSE/GRO hard X-ray data (25-1000 keV) during the X1 class event on 1991 July 18, 1425-1510 UT. GRO observations are intermittent by spacecraft night from 1430 to 1503 UT.

Between 14:40 - 14:50 UT, an intense 90 cm burst was observed to move systematically outward from the Sun with a velocity of $\approx 240 \text{ km s}^{-1}$ (Fig. 3). This outward movement is characteristic for a moving Type IV burst. 90 cm sources associated with slowly-varying emission during the decay phase of the soft X-ray burst show no systematic movement, but again, are located at heights of $h \approx 0.4R_\odot$ above the limb.

The time profile of 20 cm emission is depicted in Fig. 4 (top). Maps of the 20 cm emission during the times of maximum brightness (14:35:19 UT, 14:35:53 UT) show that the burst consists of at least two components ($T_b = 2.8 \times 10^7 \text{ K}$) which are located at heights of $h \approx 0.2R_\odot$ (Fig. 2). The PHOENIX spectrometer data reveal a “broadband, quasi-periodic pulsation event” during this period of time.

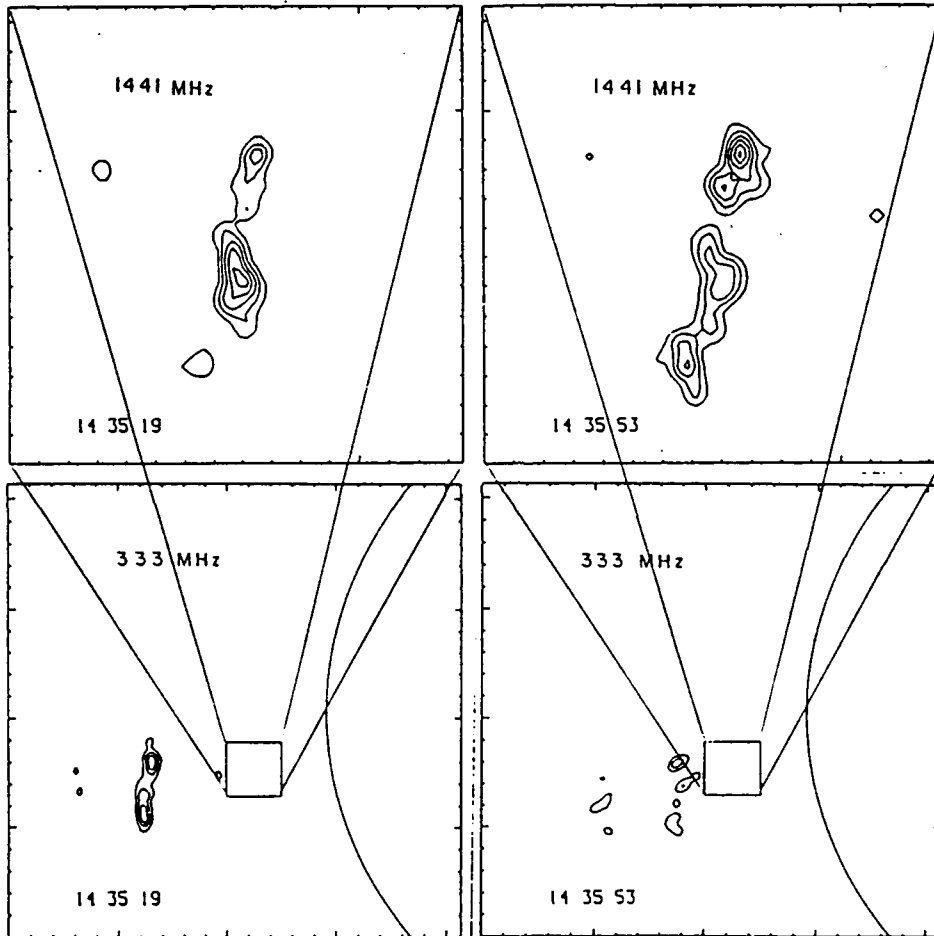


Fig. 2: VLA snapshot maps with 3.3 s time resolution of total intensity at 1441 MHz (top) and 333 MHz (bottom) at the times indicated. The contours mark levels of equal brightness temperature, with an outermost contour and contour interval of $T_b = 5.0 \times 10^6 \text{ K}$ at 1441 MHz and $T_b = 8.4 \times 10^6 \text{ K}$ at 333 MHz. The fiducial marks are drawn at intervals of $10''$ for the 1441 MHz maps, and $60''$ for the 333 MHz maps. The boxes drawn on the 333 MHz maps denote the field of view of the 1441 MHz maps.

3. PHOENIX observations

The frequency-agile PHOENIX broadband spectrometer of ETH Zurich (Switzerland) was operated in two frequency bands around the VLA frequencies 333 MHz and 1441 MHz: 20 frequencies with 3 MHz resolution in the 300-360 MHz range, and 60 frequencies with 10 MHz resolution in the 1150-1750 MHz band. The sweep spectrometer was operated with a time resolution of 40 ms. Both circular polarizations Stokes I and V are recorded, with a sensitivity of a few SFU at full time resolution. The PHOENIX spectrometer provides unique complementary information to VLA observations, such as high time resolution, broadband frequency spectra, and frequency-time drift rates.

The coregistered radio flux from VLA and PHOENIX is shown in Fig. 4 for the main flare phase, at the same frequency of 1441 MHz and with similar bandwidth (≈ 10 MHz) in both instruments. The RCP correlated flux of the shortest VLA baseline is compared with Stokes I of the full sun disk observation of PHOENIX. The broadband PHOENIX data reveal a considerable variety of radio bursts: **type III** bursts in the metric 0.30-0.35 GHz band; **type IIIdm**, **quasi-periodic pulsations**, and **intermediate drift bursts** in the decimetric 1.2-1.7 GHz band. Enlarged dynamic spectra of two episodes are displayed in Fig. 5.

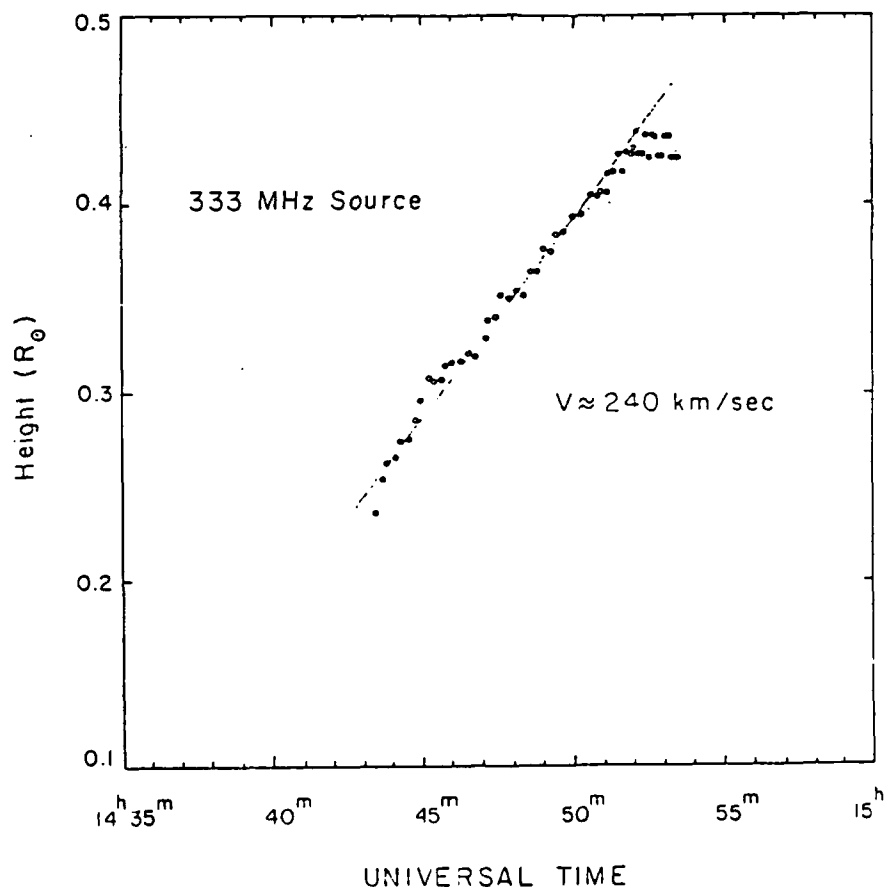


Fig. 3: A plot of height versus time for the outwardly-moving 333 MHz source shown in Figure 2. The solid line represents a constant-speed fit to the data.

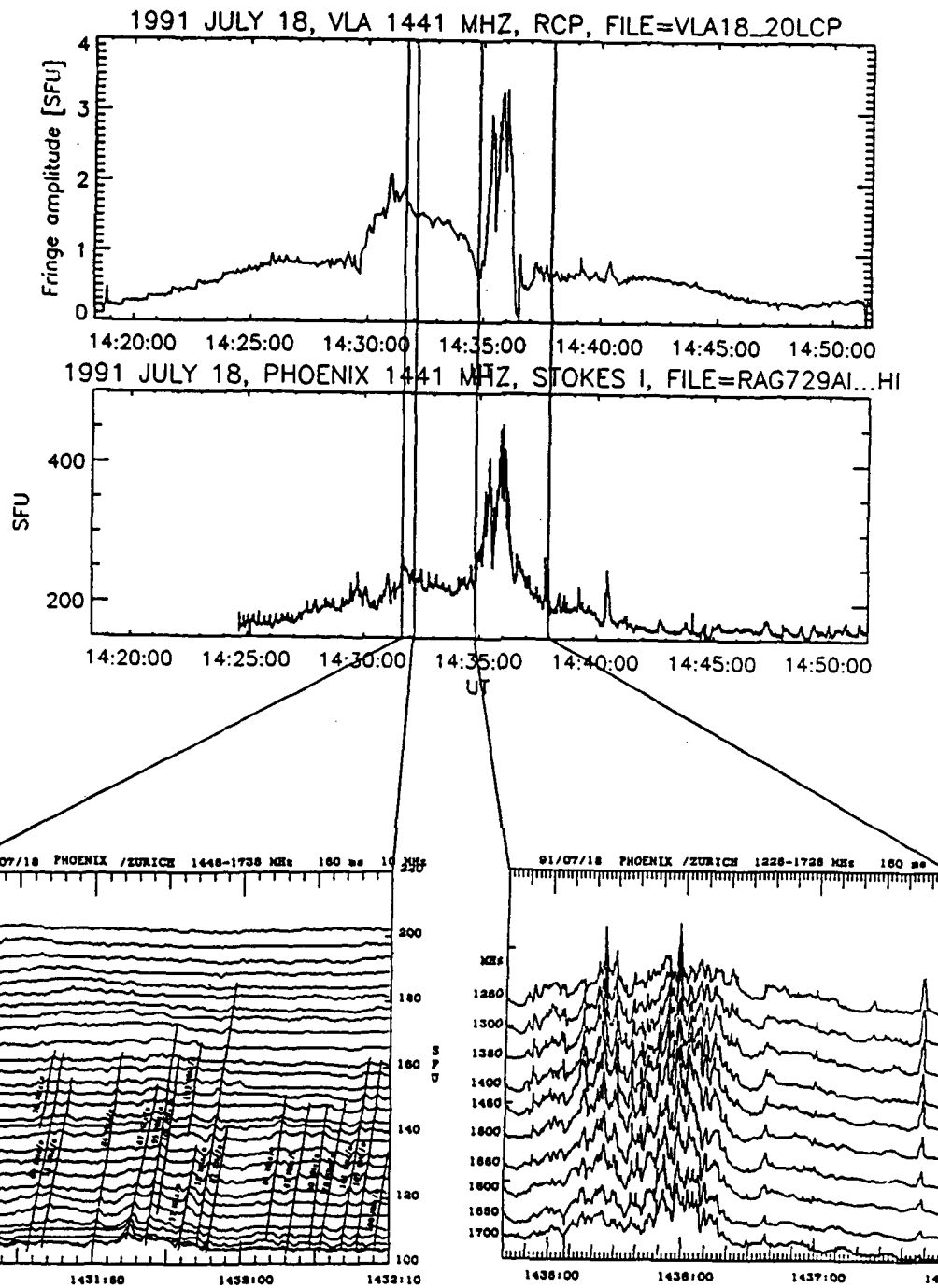


Fig. 4: Comparison of VLA (top) and PHOENIX (middle) observations at 1441 MHz. The two enlargements (bottom) show broadband dynamic spectra of the “intermediate drift bursts” (bottom left) and of the “quasi-periodic pulsation” event (bottom right). The time resolution is 3.3 s (VLA, top), 0.04 s (PHOENIX, middle), and 0.16 s (PHOENIX, bottom). Note that the brightest radio emission during the flare is related to the quasi-periodic pulsation event.

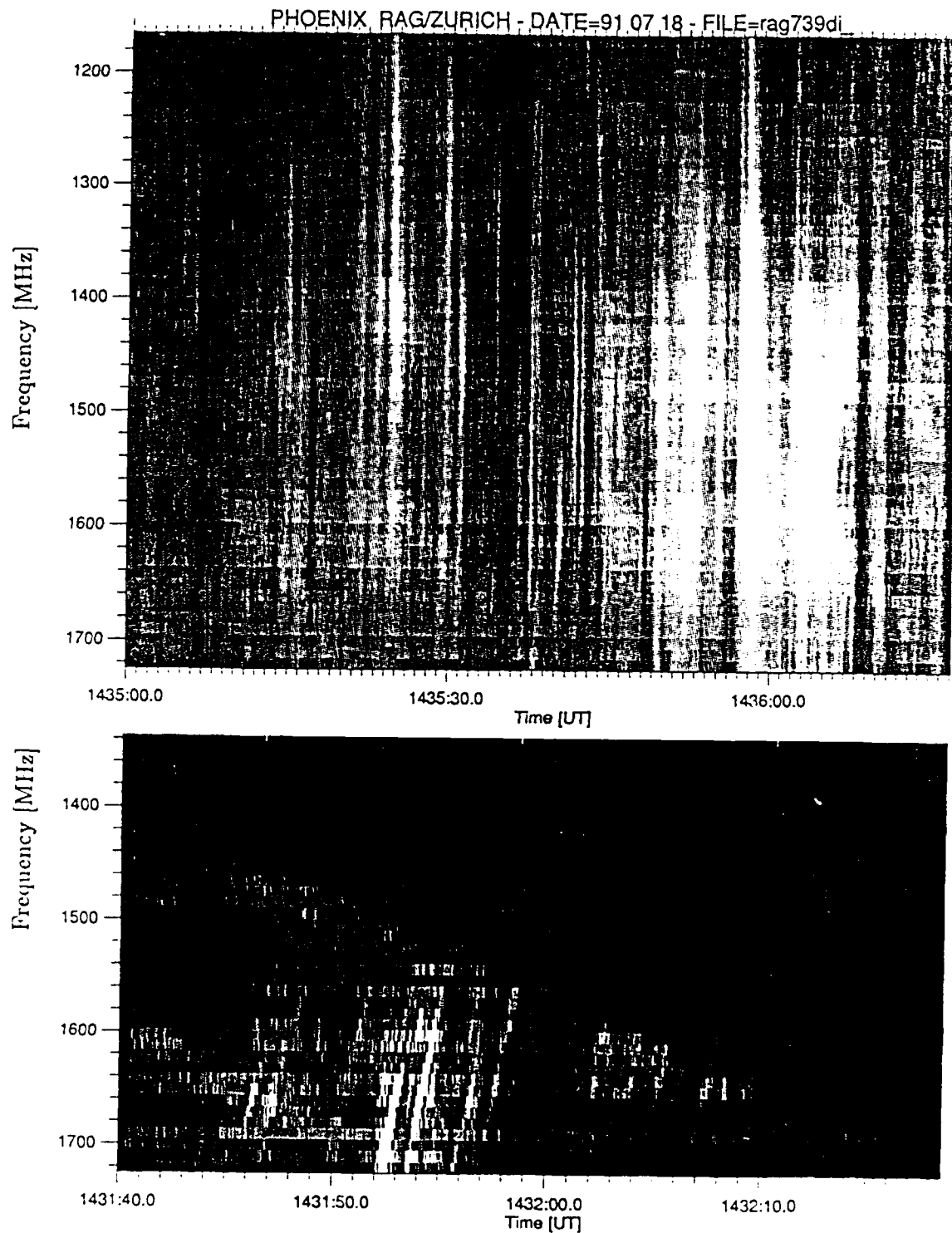


Fig. 5: PHOENIX broadband observations at 1165-1725 MHz during the impulsive phase of the X1 flare. The white color in the grayscale indicates enhanced emission. The episode of “broadband quasi-periodic pulsations” at 1435-1437 UT is shown on top. Weak “intermediate drift bursts” are visible during 1431-1432 UT (bottom).

3.1 Broadband, decimetric, quasi-periodic pulsations

The brightest radio emission at 20 cm occurs during 1435:00-1436:30 UT. While the VLA does not resolve many individual pulses, a total of about 80 pulses is identified in the PHOENIX record, with individual pulse durations of 1-2 s and frequency bandwidth of $\gtrsim 500$ MHz (Fig. 5). The frequency-time drift rate of these pulses has been measured with an automatic pattern recognition code, showing a symmetric distribution for positive and negative drift rates, where 80% of the pulses have a drift rate of $|d\nu/dt| \gtrsim 1000$ MHz/s. Monte-Carlo simulations of frequency-time drift rates with similar distributions have shown that the excitors of such radio emission originate in coronal structures with scale heights of $2 \cdot 10^3 - 2 \cdot 10^4$ km (Aschwanden and Benz, 1986). This is in good agreement with the spatial scale measured by the VLA, which is $\approx 7 \cdot 10^3$ km ($10''$) for the half width of the 20 cm emission (Fig. 2, top) during the brightest pulses. This spatial scale probably corresponds to the transverse cross-section of large loops extending to heights of $\gtrsim 0.2R_\odot$. Assuming plasma emission, the location of the 20 cm source corresponds to a density of $\gtrsim 10^{10}$ cm $^{-3}$. The time interval of the radio pulsation coincides roughly with the time of the steepest derivative in the soft X-ray time profile (Fig. 1), indicating the maximum heating rate during the flare, usually synchronized with the peak of hard X-ray emission. The characteristics of the pulsating radio time profile indicate the nonlinear dynamics of the underlying energy release mechanism (see review by Aschwanden, 1987); they cannot be explained by MHD eigen-modes which have much stricter periodicity.

3.2 Intermediate drift bursts

During the rise time of the impulsive flare phase we detected intermediate drift bursts with drift rates of ≈ -80 MHz/s (Fig 4,5). These bursts are detected for the first time in this high frequency range at 1.5-1.7 GHz. The normalized drift rate $(d\nu/dt)/\nu \approx 0.05$ is consistent with intermediate drift bursts found in the metric and decimetric range, also called "fibre" bursts. They represent a frequent fine structure of type IV bursts and can be used for diagnostics of the magnetic field. In current models they are interpreted in terms of Alfvén wave solitons (Treumann et al. 1990) or whistler wave trains (Mann et al., 1987). 3D reconstruction of the magnetic field (using the Sakurai code) and the electron density (using the diagnostics from plasma emission of simultaneously localized type III bursts) should allow us for the first time to decide between the two theoretical models and to exploit their diagnostic potential.

Acknowledgements Solar radio and X-ray studies of the Sun at Tufts University are supported by NASA grant NAGW-2383 and by grant AFOSR-89-0147 with the Air Force Office of Scientific Research. The work at NASA/GSFC was performed under grant NAS5-30442 at USRA. The VLA is operated by Associated Universities, Inc., under contract with the National Science Foundation.

References

- Aschwanden, M.J. 1987, *Sol.Phys.*, 111, 113.
- Aschwanden, M.J. and Benz, 1986, *A&A*, 158, 102.
- Mann, G., Karlicky, M., and Motschmann, U. 1987, *Sol.Phys.*, 110, 381.
- Treumann, R.A., Güdel, M. and Benz, A.O. 1990, *A&A*, 236, 242.